Hindawi
Journal of Chemistry
Volume 2017, Article ID 6897960, 9 pages
https://doi.org/10.1155/2017/6897960

Research Article

Application of Starch-Stabilized Silver Nanoparticles as a Colorimetric Sensor for Mercury(II) in 0.005 mol/L Nitric Acid

Penka Vasileva,[1] Teodora Alexandrova,[1] and Irina Karadjova[2]

[1]*Department of General and Inorganic Chemistry, Faculty of Chemistry and Pharmacy, Laboratory of Nanoparticle Science and Technology, University of Sofia "St. Kliment Ohridski", 1 J. Bourchier Blvd., 1164 Sofia, Bulgaria*
[2]*Department of Analytical Chemistry, Faculty of Chemistry and Pharmacy, University of Sofia "St. Kliment Ohridski", 1 J. Bourchier Blvd., 1164 Sofia, Bulgaria*

Correspondence should be addressed to Penka Vasileva; pvasileva@chem.uni-sofia.bg

Received 12 December 2016; Revised 13 March 2017; Accepted 28 March 2017; Published 13 April 2017

Academic Editor: Roberto Comparelli

A sensitive and selective Hg^{2+} optical sensor has been developed based on the redox interaction of Hg^{2+} with starch-coated silver nanoparticles (AgNPs) in the presence of 0.005 mol L^{-1} HNO_3. The relative intensity of the localized surface plasmon absorption band of AgNPs at 406 nm is linearly dependent on the concentration of Hg^{2+} with positive slope for the concentration range 0–12.5 $\mu g\,L^{-1}$ and negative slope for the concentration range 25–500 $\mu g\,L^{-1}$. Experiments performed demonstrated that metal ions (Na^+, K^+, Mg^{2+}, Ca^{2+}, Pb^{2+}, Cu^{2+}, Zn^{2+}, Cd^{2+}, Fe^{3+}, Co^{2+}, and Ni^{2+}) do not interfere under the same conditions, due to the absence of oxidative activity of these ions, which guarantees the high selectivity of the proposed optical sensor towards Hg^{2+}. The limits of detection and quantification were found to be 0.9 $\mu g\,L^{-1}$ and 2.7 $\mu g\,L^{-1}$, respectively, and relative standard deviations varied in the range 9–12% for Hg content from 0.9 to 12.5 $\mu g\,L^{-1}$ and 5–9% for Hg levels from 25 to 500 $\mu g\,L^{-1}$. The method was validated by analysis of CRM Estuarine Water BCR505. A possible mechanism of interaction between AgNPs and Hg^{2+} for both concentration ranges was proposed on the basis of UV-Vis, TEM, and SAED analyses.

1. Introduction

Monitoring of toxic metals in aquatic ecosystems is an important analytical task as far as these contaminants adversely affect the environment and have serious medical effects on human health. One of the most harmful pollutants among them is Hg, which is still released in the environment and widely distributed in air, water, and soil [1]. At very low concentrations, Hg affects human's health, causing a variety of diseases to the heart, kidneys, brain, and nervous and endocrine systems [2] Naturally occurring levels of mercury in groundwater and surface water are less than 0.5 $\mu g\,L^{-1}$, although local mineral deposits may produce higher levels in groundwaters. Essential quality standard for Hg maximum permissible limit of 1 $\mu g\,L^{-1}$ has been adopted at EU level and requires regular monitoring of Hg content in drinking waters. It is well known that Hg exists in natural waters as different species: Hg^0, methyl-Hg, and inorganic Hg(II); however, the dominant toxic species in drinking waters is Hg(II). Various instrumental methods and techniques have been developed for Hg determination at low environmentally relevant concentrations like atomic absorption/emission spectrometry (AAS/AES) [3], atomic fluorescence spectrometry (AFS) [4, 5], and high-performance liquid chromatography (HPLC) [6, 7]. In spite of being very sensitive and precise for Hg determination, these methods often require a time-consuming sample preparation step as well as expensive instrumentation. Various colorimetric assays (based on the use of sensitive chromophores or fluorophores [8–11], polymers [12, 13], oligonucleotides [14, 15], DNA [16, 17], and metal nanoparticles [18–20]) have been developed and reported in the literature as convenient and simple alternative methods for the detection of target analytes without the requirement of sophisticated apparatus.

Metal nanoparticles have unique properties and applications in numerous fields, which are attributed to the collective dipole oscillation known as Surface Plasmon Resonance (SPR) [21]. This phenomenon makes them very desirable

for colorimetric sensing of Hg^{2+} ions because the interaction between the nanoparticles and the analyte changes the intensity and/or position of the absorption band in the visible spectrum, which often might be observed with the naked eye [22]. The limitations observed for these systems are mainly connected with poor selectivity, high detection limit for Hg(II), complicated synthesis of the probe materials, or complicated analytical procedures.

In this study, we present a new colorimetric assay for Hg^{2+} ions in 0.005 mol L^{-1} HNO_3 using starch-stabilized silver nanoparticles (AgNPs). A change in the absorbance strength is expected as a result of the redox interaction between AgNPs and either Hg^{2+} ions or NO_3^- ions. The Hg concentration determines which of these two redox reactions dominates as the two oxidants compete with each other for Ag oxidation. This way, detection of very low environmentally relevant Hg contents is possible. Several sensing systems have been already reported based on the interaction between AgNPs and Hg(II) ions [23–32]; however, detailed study of Hg behavior in the presence of another competitive oxidant is rarely performed and discussed. A dual functional sensor for determination of Hg and H_2O_2 has been developed based on a similar approach: addition of H_2O_2 to a mixture of AgNPs and Hg(II) ions [33]. The method presented in this study, however, differs not only as a mechanism of the process, but also as a behavior of Hg^{2+} ions at very low concentrations (below 25 μg L^{-1}) towards AgNPs in the presence of NO_3^- ions as a second oxidant. A simple and fast analytical procedure for determination of Hg in drinking waters is developed and verified by the analysis of a certified reference material.

2. Materials and Methods

2.1. Apparatus. UV-Vis absorption spectra were recorded on an Evolution 300 spectrometer (Thermo Scientific, USA) within the 200–800 nm range using quartz cuvettes with 1 cm optical path length. High-purity water was used as a reference sample for background absorption. The morphology and particle sizes were examined using a high-resolution transmission electron microscope (TEM, JEOL JEM-2100 operating at an accelerating voltage of 200 kV). A volume of 5 μL AgNPs suspension was placed on a carbon-covered copper grid for TEM and air-dried. The histogram of AgNPs size distribution and the mean diameter of nanoparticles were determined by counting at least 200 nanoparticles from the different TEM images using ImageJ software. Some structural details of the nanoparticles were analyzed using the high-resolution TEM image and SAED pattern. The zeta (ζ) potential of nanoparticles was measured with a ZetaSizer Nano ZS (Malvern) instrument.

2.2. Chemicals. All chemicals used were of analytical-reagent grade and all aqueous solutions were prepared in high-purity water (Millipore Corp., Milford, MA, USA). Silver nitrate ($AgNO_3$, 99.8%), soluble starch, sodium hydroxide (NaOH, 99%), nitric acid (HNO_3, 65%), salts of the different cations studied (NaCl, KCl, $MgCl_2$, $CaCl_2$, $Pb(NO_3)_2$, $ZnCl_2$, $CuCl_2$, $NiCl_2$, $CdCl_2$, $CoCl_2$, and $FeCl_3$) (from Merck, Germany), and pharmaceutical grade D-(+) glucose (from Alfa Aesar, Germany) were used. Stock Hg standard solution, Trace CEPT™, 998 μg mL^{-1} in 2 mol L^{-1} HNO_3 (Sigma-Aldrich, USA), was used to prepare a working standard solution of 1000 μg L^{-1} Hg^{2+} in 0.01 mol L^{-1} HNO_3. Standard solutions for Hg within the concentration range of 0–1000 μg L^{-1} were prepared weekly by serial dilution of this solution in 0.01 mol L^{-1} HNO_3. All diluted Hg solutions were stored in dark glass flasks and kept refrigerated at 4°C.

2.3. Synthesis and Characterization of Silver Nanoparticles. The synthesis of AgNPs follows a green synthetic procedure as described in our previous study [34]. The silver nanoparticles were obtained through a reduction reaction of silver nitrate with D-glucose as a reducing agent in the presence of starch as a stabilizer and suitable sodium hydroxide amount as a reaction catalyst. Briefly, 24 mL of 0.001 M $AgNO_3$ and 48 mL of 0.2% solution of starch were mixed and left for at least 15 minutes to form a complex under an ultrasonic treatment (ultrasonic bath, power 100 W, frequency 38 MHz). After that, 720 μL of 0.1 M D-glucose was added and sonicated for 5 minutes. The reaction was started by the addition of 3.6 mL of 0.1 M NaOH and continued for one hour at a constant temperature (30°C) in an ultrasonic bath to ensure the homogeneous formation of the silver nanoparticles.

The as-prepared AgNPs were purified and concentrated three times by ultracentrifugation (90 min, 14,000 rpm). The dispersion obtained was denoted as a stock solution of AgNPs and used in the experiments for colorimetric determination of Hg^{2+}. The AgNPs stock solution was kept in a dark glass flask at room temperature and was homogenized in an ultrasonic bath for 30 min prior to each experiment.

2.4. Colorimetric Detection of Hg^{2+} Ions. The colorimetric detection of Hg^{2+} ions via starch-stabilized silver nanoparticles was conducted as follows: an aliquot of 200 μL AgNPs stock solution and 300 μL high-purity water were consecutively added to a small quartz cuvette, followed by addition of 500 μL Hg^{2+} solution with varying concentrations. The resulting mixture was equilibrated by stirring on Vortex for an optimum incubation time and then the UV-Vis spectrum in the wavelength range of 200–800 nm was recorded. In order to investigate the sensitivity of the colorimetric assay towards other ions, starch-stabilized AgNPs were allowed to interact under the same conditions with 50 μmol L^{-1} solutions of alkali (Na^+, K^+), alkaline earth (Mg^{2+}, Ca^{2+}), Pb^{2+}, and transition-metal ions (Cu^{2+}, Zn^{2+}, Cd^{2+}, Fe^{3+}, Co^{2+}, and Ni^{2+}) (separately for each ion). The resulting solutions were monitored by optical absorption spectroscopy.

2.5. Determination of Hg in Tap/Underground Water. Tap/underground water sample (20 mL) was filtered through a 0.45 μm filter and acidified with HNO_3 until reaching pH in the range 2–2.3. Sample aliquot of 500 μL was transferred to a quartz cuvette, and 200 μL stock solution of AgNPs was added and the mixture was stirred by the Vortex. After the incubation time of 5 min, the UV-Vis absorbance was

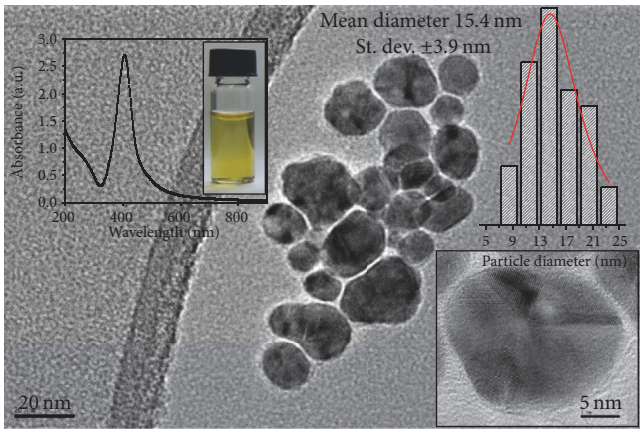

Figure 1: TEM image of starch-stabilized silver nanoparticles; insets: UV-Vis absorption spectrum and digital photographs (left), high-resolution TEM image of single nanoparticles, and histogram of nanoparticle size distribution (right).

measured at 407 nm. Parallel sample aliquot of 250 μL is diluted twice with 0.005 mol L^{-1} HNO_3 and passed through the procedure described above. The response of this sample (increase or decrease, related to the original one, Figure 4) is used to distinguish the low from the high linear concentration range of Hg and to choose an appropriate calibration curve.

3. Results and Discussion

3.1. Characterization of AgNPs. The UV-Vis absorption spectrum of starch-stabilized AgNPs, recorded at 25°C, is shown in Figure 1 (inset). A single and sharp SPR band appears at 407 nm, which indicates the formation of nanometer-sized particles. This is further confirmed by the TEM observation and size distribution histogram, shown in Figure 1.

The spherical-like AgNPs exhibit a relatively narrow size distribution with a mean diameter of 15.4 ± 3.9 nm. In addition to the nanospheres, some typical polyhedral nanoparticles (multiple twined nanocrystals) can be easily observed. The crystalline nature of AgNPs is clearly observed on the HRTEM image in Figure 1 (inset) and proved by the lattice characterization (e.g., the spacing between the individual lattice fringes of 0.235 nm, which corresponds to (111) plane lattice spacing of pure silver). The colloidal stability of starch-coated AgNPs is confirmed by the ζ-potential value of −25.3 ± 1.3 mV measured in 0.001 mol L^{-1} KCl at pH 6.8.

3.2. The Optimization of Colorimetric Sensing of Hg^{2+}. Several parameters were investigated systematically in order to establish optimal conditions for the direct colorimetric detection of Hg^{2+}. As a first step, the pH value was adjusted taking into account the analysis of real samples and HNO_3 which is typically used for water sample preservation. The experiments performed showed that 0.005 mol L^{-1} HNO_3 ensured the highest sensitivity and could be accepted as an optimal sample medium. In order to evaluate the optimum contact time, the kinetic of interaction between AgNPs and Hg^{2+} in the presence of 0.005 mol L^{-1} nitric acid was followed within one hour by measurements of UV-Vis absorbance. Typical evolution of UV-Vis absorbance spectrum with time, due to the interaction of AgNPs with 400 μg L^{-1} Hg^{2+} and respective color change of the AgNPs dispersion, is shown in Figure 2.

The changes that occurred in the LSPR absorption band of AgNPs are reflected on the color of the samples, which can be seen even with the naked eye. It is seen that the sensor's response is significant during the first five minutes of the reaction process and a negligible change in the absorption intensity is observed over time. This fact allows convenient analytical detection of Hg^{2+} within only five minutes.

As a next step, the sensitivity and applicability of starch-coated AgNPs for quantitative determination of Hg^{2+} ions under the defined optimal conditions were studied. The colorimetric response and LSPR band behavior were monitored as a function of Hg^{2+} concentrations, ranging from 0 to 500 μg L^{-1} in the presence of 0.005 mol L^{-1} HNO_3 (Figure 3).

As seen from the UV-Vis absorbance spectra (5-minute incubation time), the addition of 0.005 mol L^{-1} HNO_3 results in a considerable decrease of the intensity of AgNPs characteristic plasmon band at 407 nm accompanied by a slight blue shift (Figure 3(a)). In addition, a shoulder band appears at the wavelength range of 450–600 nm. The increase of Hg^{2+} concentration from 0 to 12.5 μg L^{-1} in 0.005 mol L^{-1} HNO_3 leads to a gradual increase of the intensity of the characteristic plasmon band of AgNPs at 407 nm and its value gradually approximates to the absorption intensity of the blank nanoparticle solution (without both NO_3^- and Hg^{2+}). In addition, the intensity of the shoulder band decreases along with increasing intensity of the main plasmon absorbance band. The spectra show a clear isosbestic point at 445 nm upon addition of Hg^{2+} in 0.005 mol L^{-1} HNO_3, demonstrating that the aggregation of AgNPs is directly related to the concentration of Hg^{2+}. Contrariwise, a gradual decrease of the intensity of the characteristic plasmon band of the AgNPs at 407 nm is observed for the Hg concentration range from 25 to 500 μg L^{-1}. The spectra presented in Figure 3(b) also show that the decrease of intensity of the absorbance maximum at 407 nm is accompanied with a slight blue shift, which is strengthened for the higher concentrations of Hg^{2+}. This phenomenon is already reported and described as a change of the refractive index of the particles and the formation of a mercury layer around AgNPs, yielding an amalgam-like structure [25, 35, 36]. It might be suggested that, for the first Hg concentration range (0–12.5 μg L^{-1}), a redox reaction proceeds between zero-valent silver (Ag^0) and either Hg^{2+} or NO_3^- ions. The values of standard electrode potentials of the components in the system confirm this suggestion: E_0 (Ag^+/Ag^0) = 0.799 V; E_0 (Hg^{2+}/Hg^0) = 0.854 V; E_0 (NO_3^-/NH_4^+) = 0.864 V. Because the standard electrode potential of NO_3^-/NH_4^+ is commeasurable with that of Hg^{2+}/Hg^0, two competitive oxidizing agents are involved in the studied sensing system. The most probable explanation for the decrease of LSPR band intensity in the presence of 0.005 mol L^{-1} HNO_3 and further increase upon addition of

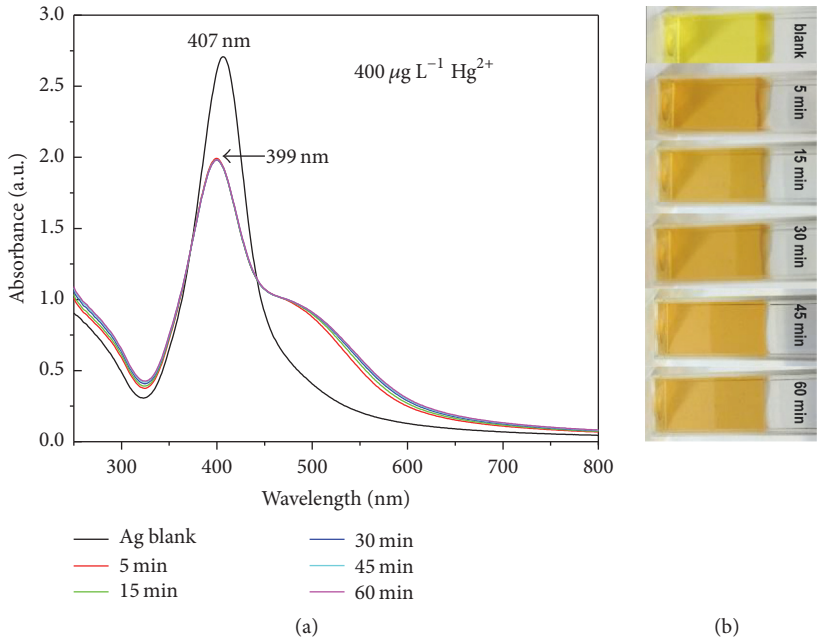

Figure 2: (a) Evolution of UV-Vis absorbance spectrum of AgNPs and (b) color change of the AgNPs dispersion upon the addition of 400 μg L^{-1} Hg^{2+} in the presence of 0.005 mol L^{-1} HNO_3.

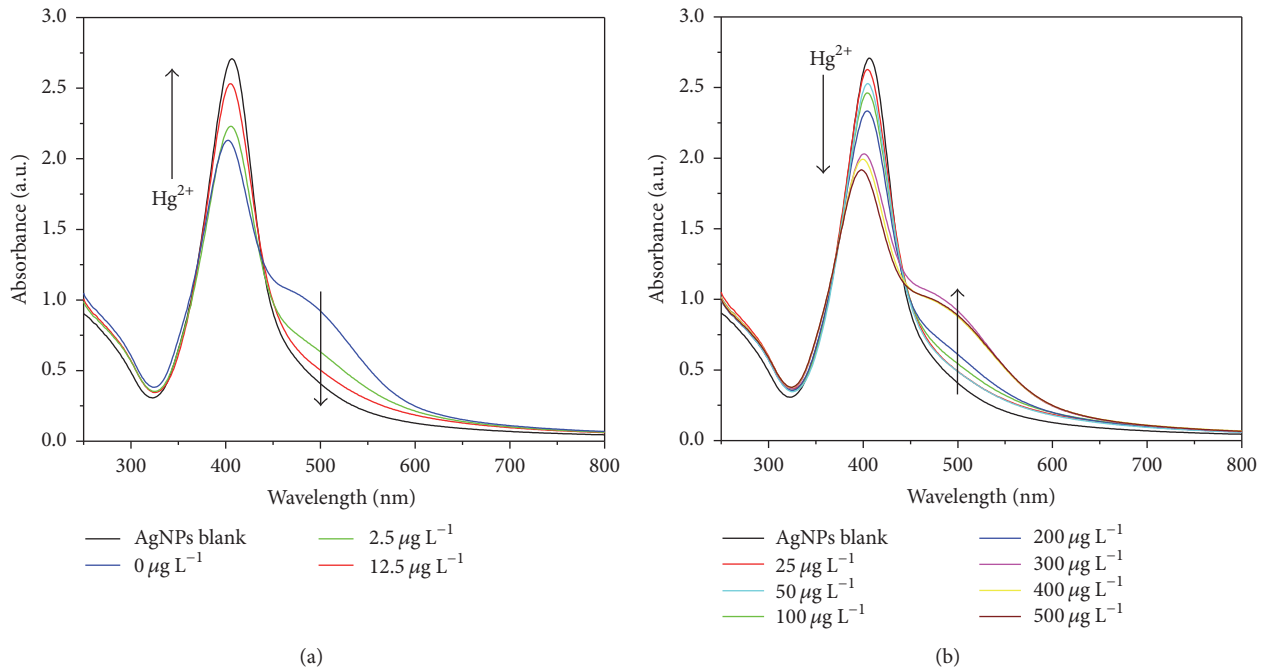

Figure 3: UV-Vis absorption responses of starch-stabilized AgNPs recorded 5 min after the addition of Hg^{2+} with various concentrations: (a) 0–12.5 μg L^{-1} Hg^{2+} and (b) 25–500 μg L^{-1} Hg^{2+} in the presence of 0.005 mol L^{-1} HNO_3.

Hg^{2+} (Figure 3(a)) is that, at low Hg^{2+} concentrations, the oxidative effect of NO_3^- ions towards surface silver atoms is dominant. In the presence of higher concentrations of Hg^{2+} (Figure 3(b)), the surface of nanoparticles is protected by the layer of Ag-Hg-amalgam due to the sorption and reduction of positively charged Hg^{2+} on the surface of negatively charged AgNPs followed by amalgamation. In this way, the surface of AgNPs is inaccessible for oxidation by NO_3^-. Evidently, within the range of 25–500 μg L^{-1} Hg^{2+}, the main redox interaction is between the AgNPs and Hg^{2+}. Such

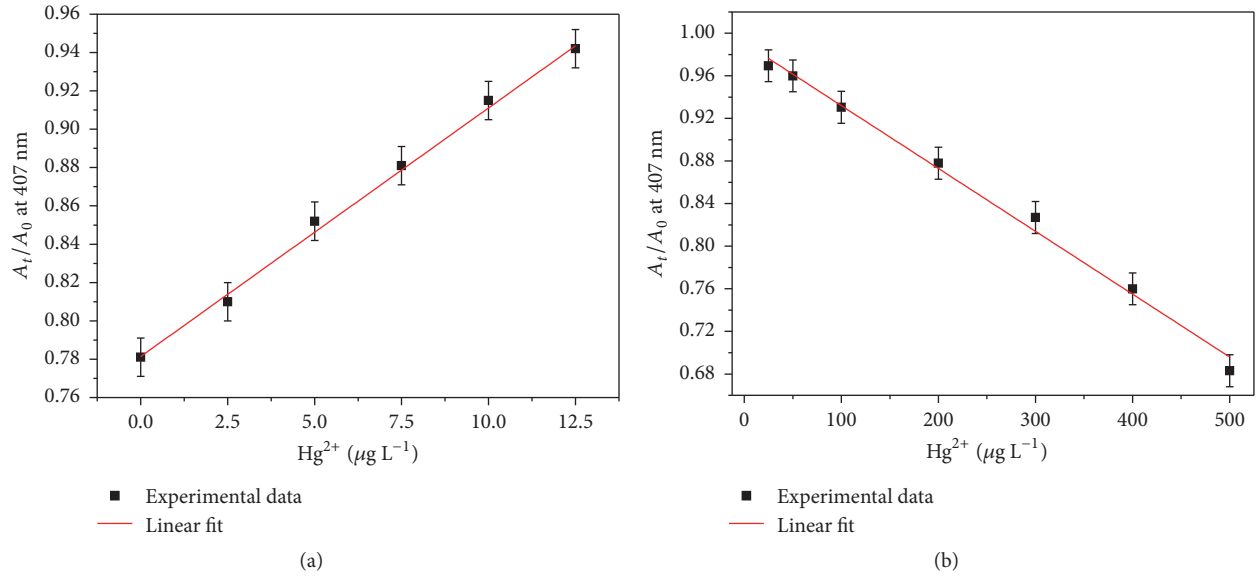

FIGURE 4: Plot of A_t/A_0 as a function of the Hg^{2+} concentration over the ranges of (a) 0–12.5 μg L^{-1} and (b) 25–500 μg L^{-1} in the presence of 0.005 mol L^{-1} HNO_3.

behavioral dissimilarities of the analyte (Hg^{2+}) for different concentration ranges have not been observed and reported in the previous studies on the AgNPs-based optical sensing system for Hg^{2+} colorimetric detection. We have to point out, however, that none of these reports mention the acidity of the reaction media, which most probably determines the oxidizing power of reagents in the system.

For quantitative determination of Hg^{2+}, the change of the intensity of LSPR band maximum of silver nanoparticles at 407 nm upon the addition of analyte with various concentrations was estimated as a ratio A_t/A_0, where A_0 corresponds to the intensity of the absorbance maximum of blank AgNPs solution (without both NO_3^- and Hg^{2+} ions) and A_t corresponds to the intensity of the absorbance maximum of silver nanoparticles 5 min after the addition of Hg^{2+} standard solutions (Figure 4).

As indicated in Figures 4(a) and 4(b), linear correlations exist between the relative value of the absorbance maximum intensity and the concentration of Hg^{2+} over the concentration ranges 0–12.5 μg L^{-1} ($\mathbf{A} = 0.7814 + 1.30 \times 10^{-2}\mathbf{c}$ with $R^2 = 0.995$) and 25–500 μg L^{-1} ($\mathbf{A} = 0.991 - 5.90 \times 10^{-4}\mathbf{c}$ with $R^2 = 0.993$), respectively. As a conclusion, the optical sensor studied using starch-stabilized AgNPs ensures a linear response over the concentration range from 0.9 to 12.5 μg L^{-1} which covers all environmentally relevant concentrations of Hg and might be used for fast screening of Hg in the aquatic environment. The second concentration range from 25 to 500 μg L^{-1} Hg^{2+} can be successfully applied for the determination of Hg in highly contaminated and rarely found industrial wastewaters.

3.3. Selectivity of Hg^{2+} Optical Sensing by Starch-Coated AgNPs. From an analytical point of view, it is very important to define the selectivity of the proposed system for colorimetric Hg^{2+} determination. This has been evaluated through the response of the assay to various environmentally relevant metal ions including Na^+, K^+, Mg^{2+}, Ca^{2+}, Pb^{2+}, Cu^{2+}, Zn^{2+}, Cd^{2+}, Fe^{3+}, Co^{2+}, and Ni^{2+} under the same conditions as in the case of Hg^{2+}. The optical response of AgNPs to the tested ions (concentration level of 50 μmol L^{-1}) after 5 min of their addition (separately for each ion) is illustrated in Figure 5. For comparison, the optical response of AgNPs to the Hg^{2+} ions at a concentration level of 2.5 μmol L^{-1} is also presented.

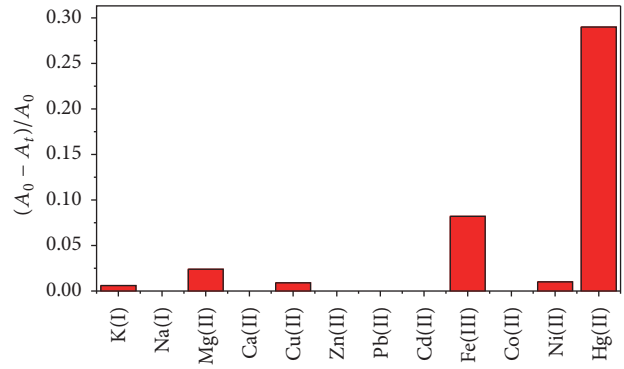

FIGURE 5: Colorimetric response of starch-stabilized AgNPs recorded 5 min after the addition of 5×10^{-5} mol L^{-1} metal ions.

It is easy to observe that all other metal ions produce a much weaker signal (almost at baseline level) except Fe^{3+} which shows modest interference. The reason is that only Hg^{2+} can be reduced by surface atoms of AgNPs to form stable Ag-Hg amalgam. The addition of Fe^{3+} resulted in a tiny intensity decrease and red shift of the absorption band. This

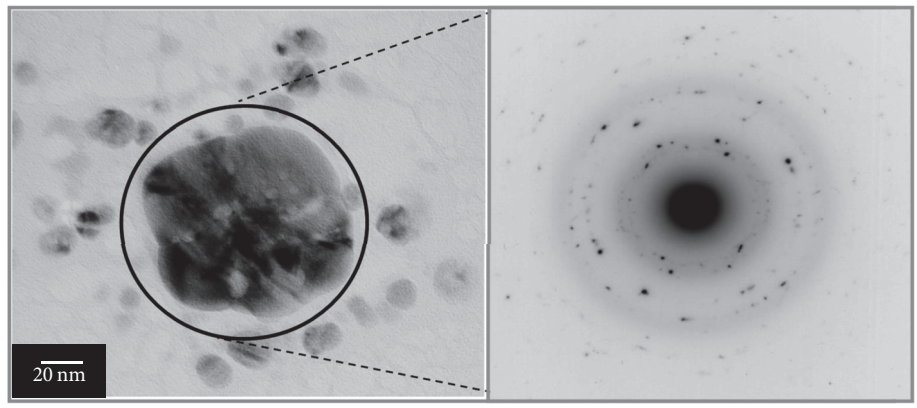

(a) (b)

Figure 6: (a) TEM image (scale bar is 20 nm) and (b) corresponding SAED pattern of starch-coated silver nanoparticles after treatment by Hg^{2+} solution at a concentration of 500 $\mu g\,L^{-1}$ in the presence of 0.005 mol L^{-1} HNO_3.

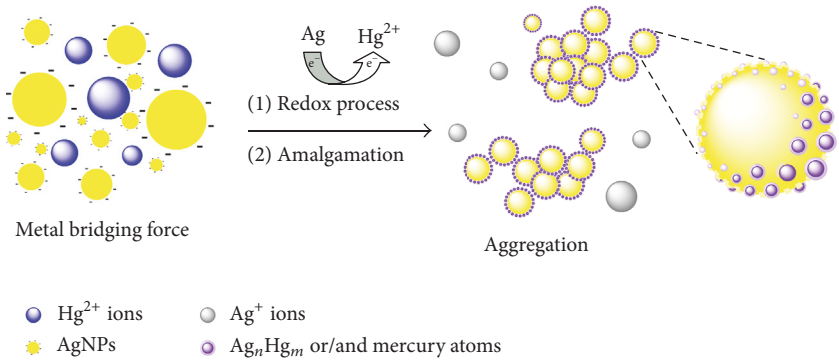

Figure 7: The proposed mechanism of the interaction between starch-coated AgNPs and Hg^{2+} solution.

effect could be interpreted in terms of Fe(III) complexation with oxidized species of carbohydrates (starch and glucose) which are sorbed on the surface of silver nanoparticles [37].

3.4. Mechanism of Interaction between AgNPs and Hg^{2+}. To elucidate the mechanism of sensing activity of the starch-coated AgNPs towards Hg^{2+}, the nanoparticles were examined before and after Hg^{2+} exposure using TEM with SAED observations. Figure 6 shows TEM micrograph with the corresponding SAED pattern obtained from the agglomerate formed during interaction of AgNPs with Hg^{2+} solution at a concentration of 500 $\mu g\,L^{-1}$.

As can be seen from Figure 6(a), the nanoparticles are of varying sizes and there is a large distribution after Hg^{2+} exposure. The TEM image shows a larger particle, which is surrounded by smaller particles. It seems that larger particles are undergoing Ostwald ripening. A similar observation is already reported for gold nanoparticles utilized for mercury removal from drinking water [38] and for colorimetric detection of Hg^{2+} using the AgNPs embedded in cyclodextrin-silicate composite [39].

The data from the analysis of SAED pattern (Figure 6(b)) are summarized with interpretation accuracy of 1% in Table 1. The analysis shows the existence of Ag_2Hg_3 amalgam (PDF 65-3156) and Ag (PDF 89-3722) as main phases in the aggregated mass formed during the interaction of starch-coated AgNPs with Hg^{2+}. Some impurities of metallic Hg (PDF 01-1017) are also detected.

On the basis of TEM/SAED results, a multistep interaction of Hg^{2+} with the silver nanoparticles could be inferred. The interaction involves (i) the electrostatic attraction between negatively charged silver nanoparticles and positively charged Hg^{2+} species, decreasing the distance between nanoparticles; (ii) adsorption of Hg^{2+} on the surface of AgNPs and their reduction to Hg^0 by the surface Ag atoms (simultaneously obtained Ag^+ diffuse into the solution); (iii) amalgamation of the freshly generated mercury atoms with the surface Ag atoms [25, 32, 39]; (iv) the interaction of Hg^{2+} with AgNPs which decreases surface charges of nanoparticles, leading to their destabilization and aggregation. The latter one is confirmed by the shape evolution of AgNPs observed in Figure 6(a). The suggested mechanism of optical sensing of Hg^{2+} by starch-coated silver nanoparticles is illustrated in Figure 7.

3.5. Analytical Application. In order to test the applicability of the sensor developed for Hg^{2+} and total Hg determination, samples of tap water (Sofia) and mineral water (Gorna Bania,

Table 1: SAED data of AgNPs aggregates formed after exposure of silver nanoparticles to Hg^{2+} at concentration of 500 $\mu g\,L^{-1}$ in the presence of 0.005 mol L^{-1} HNO_3. $(hkl)_f$: double electron diffraction effects; SAED interpretation: accuracy 1%.

d (Å)	Relative intensity	Ag PDF 89-3722 a = 4.0855(1) Å SG $Fm\bar{3}m$	Ag PDF 87-0598 a = 2.8862 Å, c = 10.000 Å $P6_3/mmc$	Ag_2Hg_3 PDF 65-3156 a = 10.0506 Å SG I23
2.438	s	—	101	$(410)_f$
2.136	s	—	—	332
1.506	s	—	—	622
1.287	s	$(310)_f$	—	237
1.057	w	—	205	930
0.979	w	$(410)_f$	—	059

s: strong; w: weak.

Table 2: Comparison of different methods using silver nanoparticles as a colorimetric sensing probe for Hg^{2+} determination.

Sensing probe	Linear concentration range	Detection limit	Ref.
Starch-stabilized AgNPs	50 nmol L^{-1}–5000 nmol L^{-1}	25 nmol L^{-1}	[23]
Unmodified AgNPs stabilized with extract of soap-root plant	10–100 μmol L^{-1}	2.2 μmol L^{-1}	[26]
Gum kondagogu-stabilized AgNPs	50–500 nmol L^{-1}	50 nmol L^{-1} (LOQ)	[31]
Citrate-capped AgNPs	0.02 nmol L^{-1}–0.9 μmol L^{-1}	—	[33]
1-Dodecanethiol-capped Ag nanoprisms upon the presence of iodides	10–4000 nmol L^{-1}	3.3 nmol L^{-1}	[40]
Poly(vinylpyrrolidone)-stabilized AgNPs	1 nmol L^{-1}–30 μmol L^{-1}	1 nmol L^{-1}	[41]
Carrageenan-functionalized Ag/AgCl NPs	1–100 μmol L^{-1}	1 μmol L^{-1}	[42]
Starch-coated AgNPs in the presence of 0.005 mol L^{-1} HNO_3	4.5–2500 nmol L^{-1}	4.5 nmol L^{-1}	This work

Kniagevo) were spiked at levels close to the permissible limit (drinking water) of 1 $\mu g\,L^{-1}$. Total Hg content in these samples was defined preliminarily by ICP-MS and results for all samples were below 0.05 $\mu g\,L^{-1}$ Hg. Recoveries achieved using the described procedure are in the range 93–97%, thus confirming the possibility of fast Hg^{2+} screening in drinking waters using the proposed sensor based on starch-coated AgNPs. The limits of detection (LOD) and limits of quantification (LOQ) were evaluated on the basis of repeated analysis of blank (AgNPs). The calculations were based on 3σ and 10σ criteria using the linear regression equations and slopes of calibration graphs for Hg^{2+} (Figure 4). The defined values for LOD (0.9 $\mu g\,L^{-1}$) and LOQ (2.7 $\mu g\,L^{-1}$) show that the proposed sensor is not suitable for surface water monitoring but might be successfully used for fast *on-site* control of the quality of sources for drinking water. Within-batch precision strongly depends on the analyte concentration in the measuring solution: 9–12% for Hg^{2+} in the range 0.9–12.5 $\mu g\,L^{-1}$ and 5–9% for Hg^{2+} in the range over 25–500 $\mu g\,L^{-1}$. Table 2 further summarizes the linear ranges and detection limits of various Hg^{2+} detection methods based on silver nanoparticles as a colorimetric sensing probe. It is evident that the proposed method ensures higher or equal sensitivity with those of earlier reported colorimetric AgNPs-based sensors [23, 26, 31, 33, 40–42].

For partial validation of the procedure, CRM Estuarine Water BCR505 was analyzed after solid phase extraction (10-fold Hg enrichment) [43]. Three sample aliquots of 800 μL were analyzed according to the proposed analytical procedure. The result of 0.73 ± 0.08 nmol L^{-1} Hg was in reasonable agreement with the (additional material information) value of 0.69 nmol kg^{-1} Hg (138 $\mu g\,L^{-1}$).

4. Conclusions

A simple, fast, and low cost analytical procedure is developed for easy and sensitive quantification of Hg^{2+} in the presence of 0.005 mol L^{-1} HNO_3 by using starch-coated AgNPs as a LSPR-based optical sensor. The Hg^{2+} sensing is based on the optical response (change in the absorbance strength of LSPR band) of silver nanoparticles depending on the Hg^{2+} concentration. Possible mechanism of interaction between

AgNPs and Hg^{2+} was proposed. An accurate and reliable determination of Hg is achieved in two concentration ranges: 0.9–12.5 $\mu g\,L^{-1}$ and 25–500 $\mu g\,L^{-1}$. The limits of detection and quantification achieved were 0.9 $\mu g\,L^{-1}$ and 2.7 $\mu g\,L^{-1}$, respectively, and relative standard deviations varied in the range 9–12% for Hg content from 0.9 to 12.5 $\mu g\,L^{-1}$ and 5–9% for Hg levels from 25 to 500 $\mu g\,L^{-1}$. The LSPR-based optical sensor for Hg(II) might be used for simple and fast *on-site* screening of sources for abstraction of drinking water and for Hg determination in wastewaters.

Conflicts of Interest

The authors declare that there are no conflicts of interest regarding the publication of this paper.

Acknowledgments

The authors acknowledge the support by the Horizon 2020 program of the European Commission (project Materials Networking).

References

[1] D. W. Boening, "Ecological effects, transport, and fate of mercury: a general review," *Chemosphere*, vol. 40, no. 12, pp. 1335–1351, 2000.

[2] P. Holmes, K. A. F. James, and L. S. Levy, "Is low-level environmental mercury exposure of concern to human health?" *Science of the Total Environment*, vol. 408, no. 2, pp. 171–182, 2009.

[3] H. Erxleben and J. Ruzicka, "Atomic absorption spectroscopy for mercury, automated by sequential injection and miniaturized in lab-on-valve system," *Analytical Chemistry*, vol. 77, no. 16, pp. 5124–5128, 2005.

[4] L.-P. Yu and X.-P. Yan, "Flow injection on-line sorption preconcentration coupled with cold vapor atomic fluorescence spectrometry and on-line oxidative elution for the determination of trace mercury in water samples," *Atomic Spectroscopy*, vol. 25, no. 3, pp. 145–153, 2004.

[5] M. J. Bloxham, S. J. Hill, and P. J. Worsfold, "Determination of mercury in filtered sea-water by flow injection with on-line oxidation and atomic fluorescence spectrometric detection," *Journal of Analytical Atomic Spectrometry*, vol. 11, no. 7, pp. 511–514, 1996.

[6] M. Lombardo, I. Vassura, D. Fabbri, and C. Trombini, "A strikingly fast route to methylmercury acetylides as a new opportunity for monomethylmercury detection," *Journal of Organometallic Chemistry*, vol. 690, no. 3, pp. 588–593, 2005.

[7] L. Liu, Y.-W. Lam, and W.-Y. Wong, "Complexation of 4,4′-di(*tert*-butyl)-5-ethynyl-2,2′-bithiazole with mercury(II) ion: synthesis, structures and analytical applications," *Journal of Organometallic Chemistry*, vol. 691, no. 6, pp. 1092–1100, 2006.

[8] A. Caballero, R. Martínez, V. Lloveras et al., "Highly selective chromogenic and redox or fluorescent sensors of Hg^{2+} in aqueous environment based on 1,4-disubstituted azines," *Journal of the American Chemical Society*, vol. 127, no. 45, pp. 15666–15667, 2005.

[9] H. Zheng, Z.-H. Qian, L. Xu, F.-F. Yuan, L.-D. Lan, and J.-G. Xu, "Switching the recognition preference of rhodamine B spirolactam by replacing one atom: design of rhodamine B thiohydrazide for recognition of Hg(II) in aqueous solution," *Organic Letters*, vol. 8, no. 5, pp. 859–861, 2006.

[10] Y. Zhao and Z. Zhong, "Tuning the sensitivity of a foldamer-based mercury sensor by its folding energy," *Journal of the American Chemical Society*, vol. 128, no. 31, pp. 9988–9989, 2006.

[11] H. Wang, Y. Wang, J. Jin, and R. Yang, "Gold nanoparticle-based colorimetric and "turn-on" fluorescent probe for mercury(II) ions in aqueous solution," *Analytical Chemistry*, vol. 80, no. 23, pp. 9021–9028, 2008.

[12] X. Liu, Y. Tang, L. Wang et al., "Optical detection of mercury(II) in aqueous solutions by using conjugated polymers and label-free oligonucleotides," *Advanced Materials*, vol. 19, no. 11, pp. 1471–1474, 2007.

[13] I.-B. Kim and U. H. F. Bunz, "Modulating the sensory response of a conjugated polymer by proteins: an agglutination assay for mercury ions in water," *Journal of the American Chemical Society*, vol. 128, no. 9, pp. 2818–2819, 2006.

[14] S.-J. Liu, H.-G. Nie, J.-H. Jiang, G.-L. Shen, and R.-Q. Yu, "Electrochemical sensor for mercury(II) based on conformational switch mediated by interstrand cooperative coordination," *Analytical Chemistry*, vol. 81, no. 14, pp. 5724–5730, 2009.

[15] Z. Zhu, Y. Su, J. Li et al., "Highly sensitive electrochemical sensor for mercury(II) ions by using a mercury-specific oligonucleotide probe and gold nanoparticle-based amplification," *Analytical Chemistry*, vol. 81, no. 18, pp. 7660–7666, 2009.

[16] D. Zhang, M. Deng, L. Xu, Y. Zhou, J. Yuwen, and X. Zhou, "The sensitive and selective optical detection of mercury(II) ions by using a phosphorothioate DNAzyme strategy," *Chemistry—A European Journal*, vol. 15, no. 33, pp. 8117–8120, 2009.

[17] M. Hollenstein, C. Hipolito, C. Lam, D. Dietrich, and D. M. Perrin, "A highly selective DNAzyme sensor for mercuric ions," *Angewandte Chemie—International Edition*, vol. 47, no. 23, pp. 4346–4350, 2008.

[18] M. Rex, F. E. Hernandez, and A. D. Campiglia, "Pushing the limits of mercury sensors with gold nanorods," *Analytical Chemistry*, vol. 78, no. 2, pp. 445–451, 2006.

[19] Y. Wang, F. Yang, and X. Yang, "Colorimetric detection of mercury(II) ion using unmodified silver nanoparticles and mercury-specific oligonucleotides," *ACS Applied Materials and Interfaces*, vol. 2, no. 2, pp. 339–342, 2010.

[20] Y.-R. Kim, R. K. Mahajan, J. S. Kim, and H. Kim, "Highly sensitive gold nanoparticle-based colorimetric sensing of mercury(II) through simple ligand exchange reaction in aqueous media," *ACS Applied Materials and Interfaces*, vol. 2, no. 1, pp. 292–295, 2010.

[21] D. V. Talapin, J.-S. Lee, M. V. Kovalenko, and E. V. Shevchenko, "Prospects of colloidal nanocrystals for electronic and optoelectronic applications," *Chemical Reviews*, vol. 110, no. 1, pp. 389–458, 2010.

[22] Y.-L. Hung, T.-M. Hsiung, Y.-Y. Chen, Y.-F. Huang, and C.-C. Huang, "Colorimetric detection of heavy metal ions using label-free gold nanoparticles and alkanethiols," *The Journal of Physical Chemistry C*, vol. 114, no. 39, pp. 16329–16334, 2010.

[23] Y. Fan, Z. Liu, L. Wang, and J. Zhan, "Synthesis of starch-stabilized Ag nanoparticles and Hg^{2+} recognition in aqueous media," *Nanoscale Research Letters*, vol. 4, no. 10, pp. 1230–1235, 2009.

[24] G. V. Ramesh and T. P. Radhakrishnan, "A universal sensor for mercury (Hg, Hg^{I}, Hg^{II}) based on silver nanoparticle-embedded polymer thin film," *ACS Applied Materials & Interfaces*, vol. 3, pp. 988–994, 2011.

[25] E. Sumesh, M. S. Bootharaju, Anshup, and T. Pradeep, "A practical silver nanoparticle-based adsorbent for the removal of Hg^{2+} from water," *Journal of Hazardous Materials*, vol. 189, no. 1-2, pp. 450–457, 2011.

[26] K. Farhadi, M. Forough, R. Molaei, S. Hajizadeh, and A. Rafipour, "Highly selective Hg^{2+} colorimetric sensor using green synthesized and unmodified silver nanoparticles," *Sensors and Actuators B: Chemical*, vol. 161, no. 1, pp. 880–885, 2012.

[27] G. Maduraiveeran and R. Ramaraj, "Enhanced sensing of mercuric ions based on dinucleotide-functionalized silver nanoparticles," *Analytical Methods*, vol. 8, no. 44, pp. 7966–7971, 2016.

[28] A. Jeevika and D. R. Shankaran, "Functionalized silver nanoparticles probe for visual colorimetric sensing of mercury," *Materials Research Bulletin*, vol. 83, pp. 48–55, 2016.

[29] Y. Ma, Y. Pang, F. Liu, H. Xu, and X. Shen, "Microwave-assisted ultrafast synthesis of silver nanoparticles for detection of Hg^{2+}," *Spectrochimica Acta Part A: Molecular and Biomolecular Spectroscopy*, vol. 153, pp. 206–211, 2016.

[30] Z. Guo, G. Chen, G. Zeng et al., "Ultrasensitive detection and co-stability of mercury(II) ions based on amalgam formation with Tween 20-stabilized silver nanoparticles," *RSC Advances*, vol. 4, no. 103, pp. 59275–59283, 2014.

[31] L. Rastogi, R. B. Sashidhar, D. Karunasagar, and J. Arunachalam, "Gum kondagogu reduced/stabilized silver nanoparticles as direct colorimetric sensor for the sensitive detection of Hg^{2+} in aqueous system," *Talanta*, vol. 118, pp. 111–117, 2014.

[32] S. S. Ravi, L. R. Christena, N. Saisubramanian, and S. P. Anthony, "Green synthesized silver nanoparticles for selective colorimetric sensing of Hg^{2+} in aqueous solution at wide pH range," *Analyst*, vol. 138, no. 15, pp. 4370–4377, 2013.

[33] G.-L. Wang, X.-Y. Zhu, H.-J. Jiao, Y.-M. Dong, and Z.-J. Li, "Ultrasensitive and dual functional colorimetric sensors for mercury (II) ions and hydrogen peroxide based on catalytic reduction property of silver nanoparticles," *Biosensors and Bioelectronics*, vol. 31, no. 1, pp. 337–342, 2012.

[34] P. Vasileva, B. Donkova, I. Karadjova, and C. Dushkin, "Synthesis of starch-stabilized silver nanoparticles and their application as a surface plasmon resonance-based sensor of hydrogen peroxide," *Colloids and Surfaces A: Physicochemical and Engineering Aspects*, vol. 382, no. 1–3, pp. 203–210, 2011.

[35] P. Mulvaney, "Surface plasmon spectroscopy of nanosized metal particles," *Langmuir*, vol. 12, no. 3, pp. 788–800, 1996.

[36] T. Morris, H. Copeland, E. McLinden, S. Wilson, and G. Szulczewski, "The effects of mercury adsorption on the optical response of size-selected gold and silver nanoparticles," *Langmuir*, vol. 18, no. 20, pp. 7261–7264, 2002.

[37] S. Komulainen, J. Pursiainen, P. Perämäki, and M. Lajunen, "Complexation of Fe(III) with water-soluble oxidized starch," *Starch*, vol. 65, no. 3-4, pp. 338–345, 2013.

[38] K. P. Lisha, Anshup, and T. Pradeep, "Towards a practical solution for removing inorganic mercury from drinking water using gold nanoparticles," *Gold Bulletin*, vol. 42, no. 2, pp. 144–152, 2009.

[39] S. Manivannan and R. Ramaraj, "Silver nanoparticles embedded in cyclodextrin-silicate composite and their applications in Hg(II) ion and nitrobenzene sensing," *Analyst*, vol. 138, no. 6, pp. 1733–1739, 2013.

[40] L. Chen, X. Fu, W. Lu, and L. Chen, "Highly sensitive and selective colorimetric sensing of Hg^{2+} based on the morphology transition of silver nanoprisms," *ACS Applied Materials and Interfaces*, vol. 5, no. 2, pp. 284–290, 2013.

[41] L. Li, L. Gui, and W. Li, "A colorimetric silver nanoparticle-based assay for Hg(II) using lysine as a particle-linking reagent," *Microchimica Acta*, vol. 182, no. 11-12, pp. 1977–1981, 2015.

[42] K. B. Narayanan and S. S. Han, "Highly selective and quantitative colorimetric detection of mercury(II) ions by carrageenan-functionalized Ag/AgCl nanoparticles," *Carbohydrate Polymers*, vol. 160, pp. 90–96, 2017.

[43] E. K. Mladenova, I. G. Dakova, D. L. Tsalev, and I. B. Karadjova, "Mercury determination and speciation analysis in surface waters," *Central European Journal of Chemistry*, vol. 10, no. 4, pp. 1175–1182, 2012.